

## **Supplemental Data**

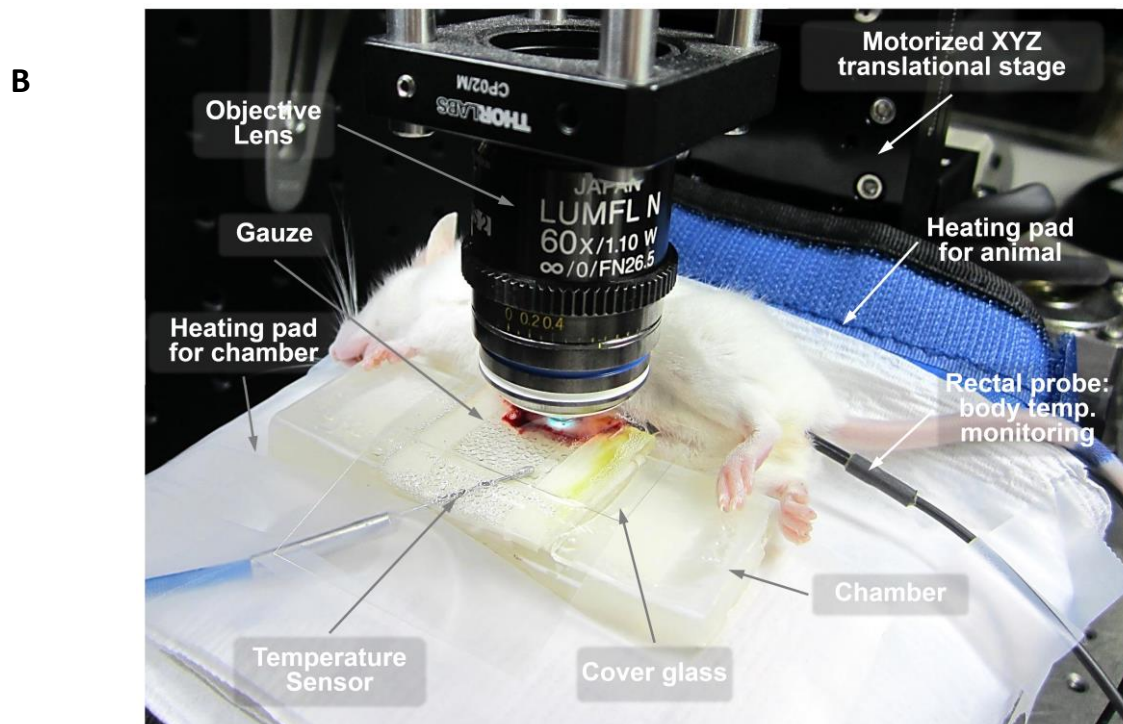
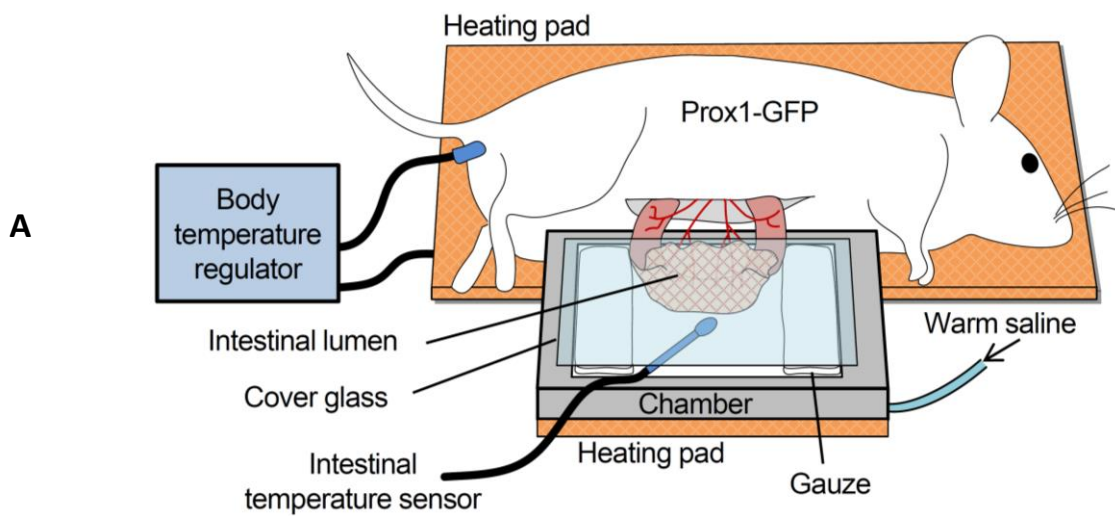
### **Intravital imaging of intestinal lacteal unveils lipid drainage through contractility**

Kibaek Choe, Jeon Yeob Jang, Intae Park, Yeseul Kim, Soyeon Ahn, Dae-Young Park, Young-Kwon Hong, Kari Alitalo, Gou Young Koh and Pilhan Kim

#### **Contents:**

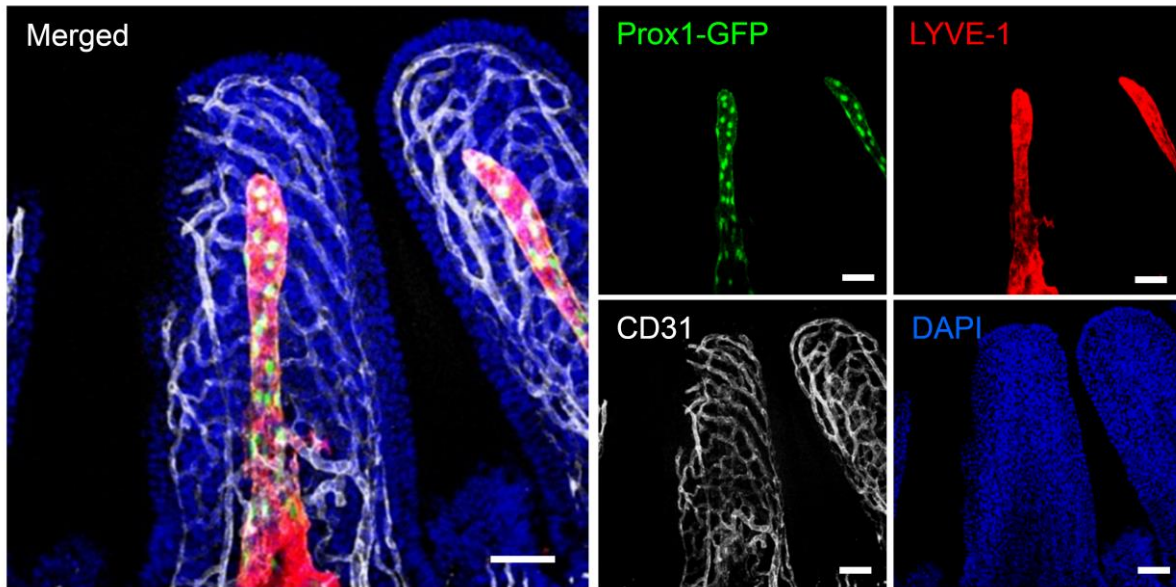
Supplemental Figures 1-9

Supplemental Movies 1-7

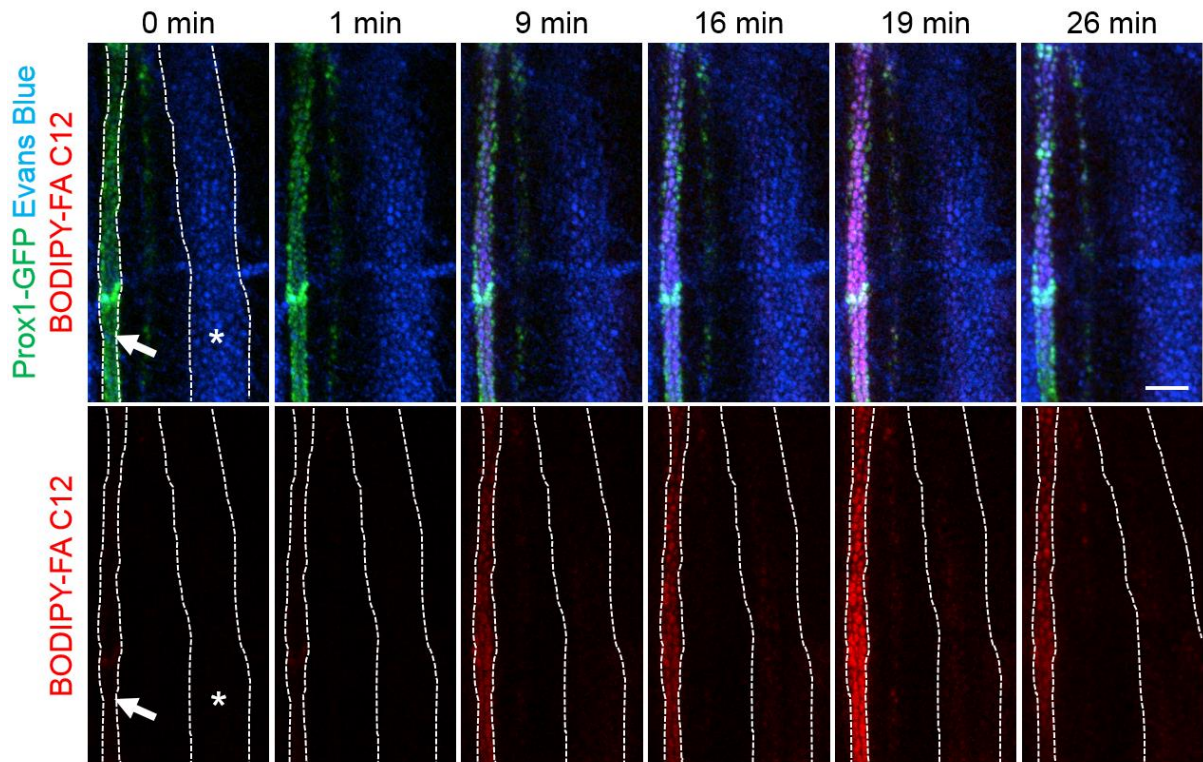


**Supplemental Figure 1. Mouse preparation for intravital imaging of small intestinal villi.**

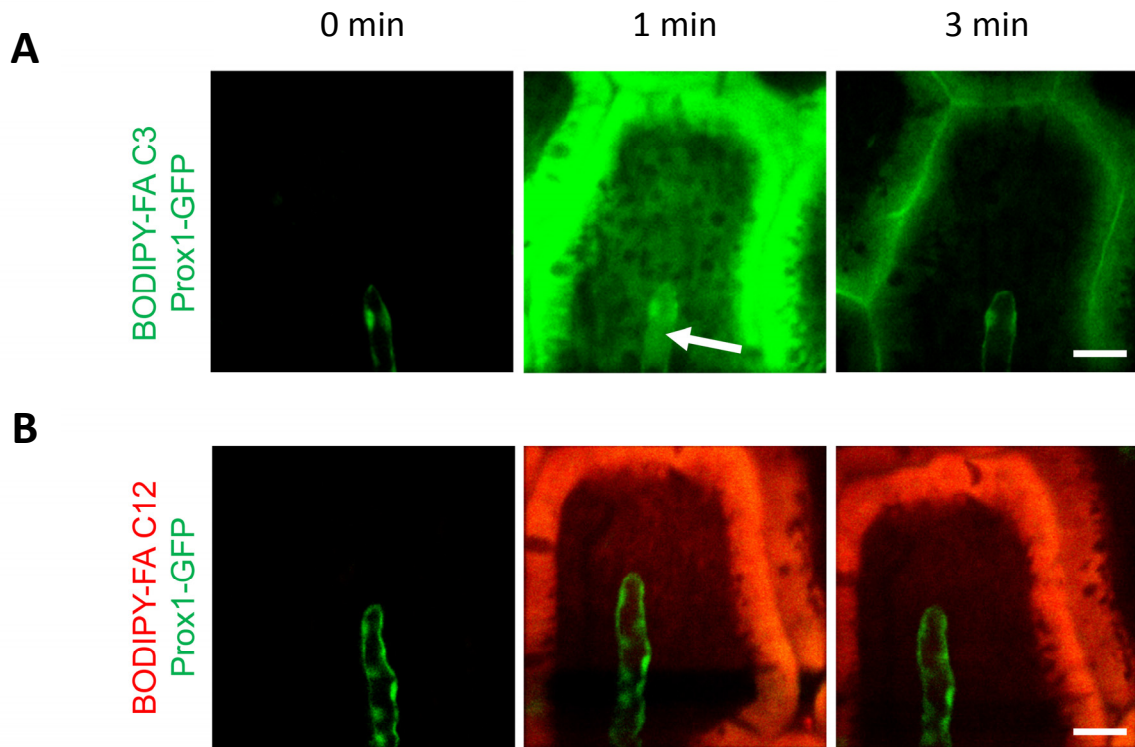
Exteriorized intestinal lumen is placed in a chamber filled with wet gauze and covered with a cover glass. Chamber temperature and the body temperature of anesthetized mice are maintained at 37 °C by a heating pad with temperature sensor and a body temperature regulator with rectal probe, respectively.



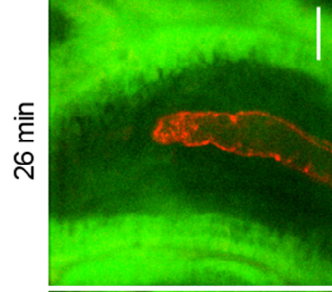
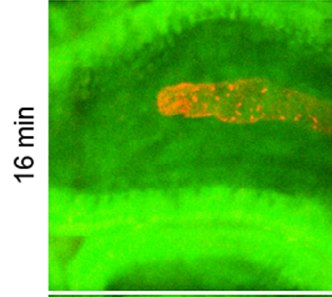
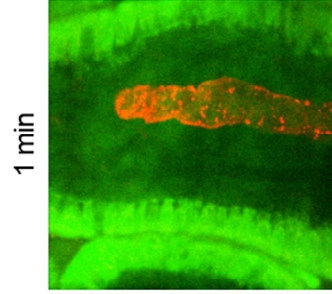
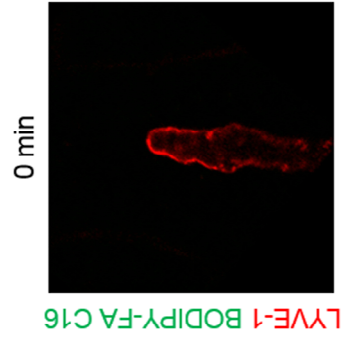
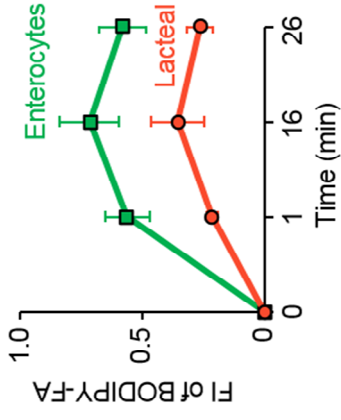
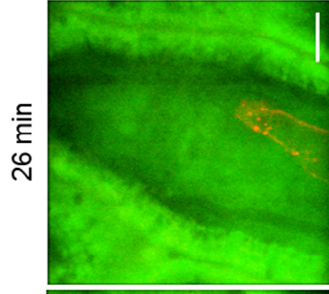
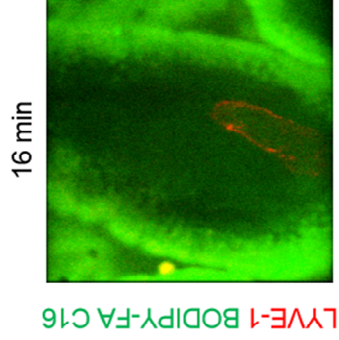
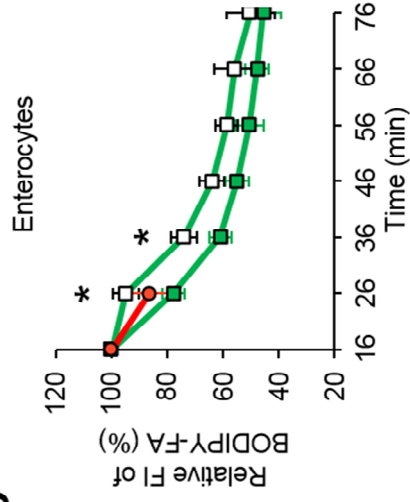
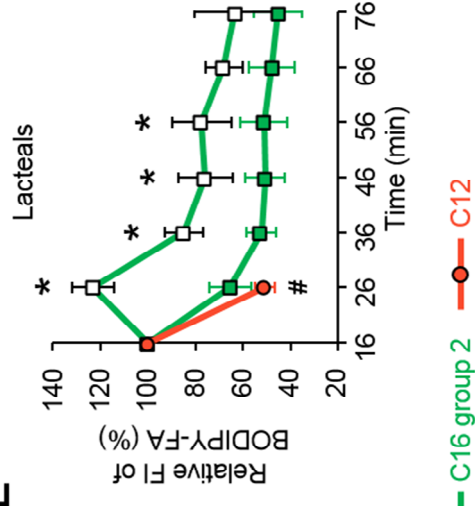
**Supplemental Figure 2. Images showing lacteal structure visualized with the fluorescent signals from Prox1-GFP mice. Scale bars, 50  $\mu$ m.**



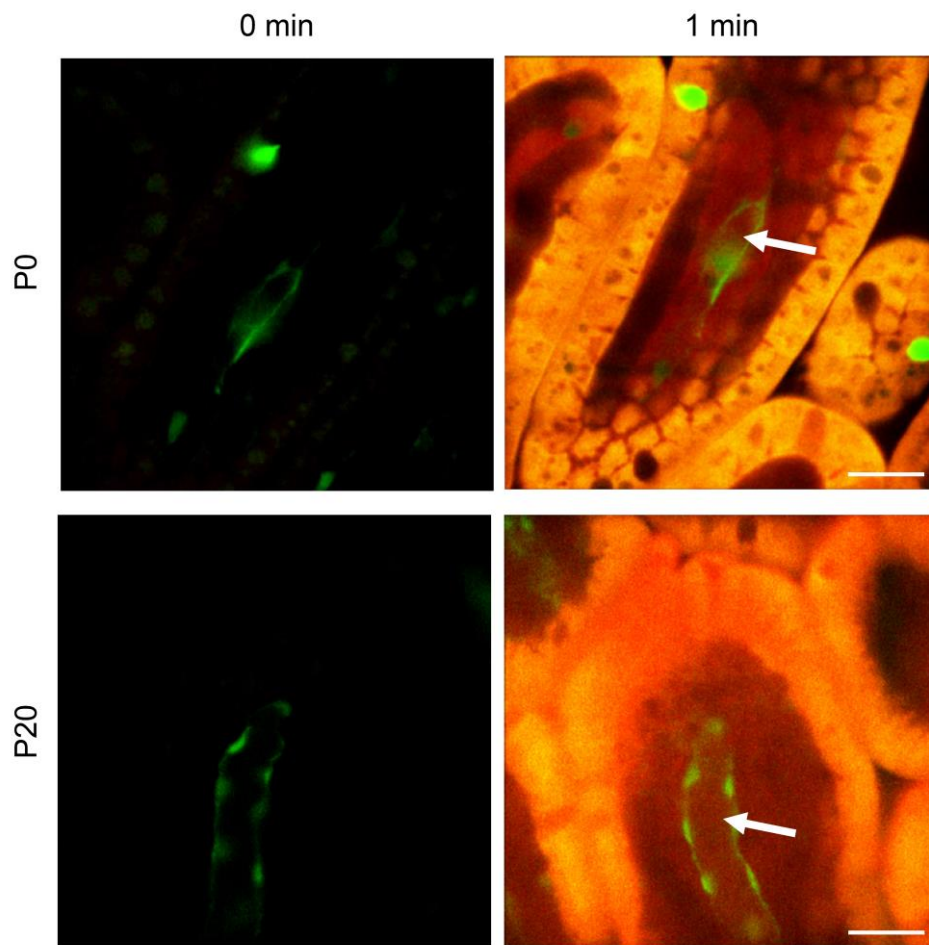
**Supplemental Figure 3. Validation of lacteal imaging chamber system by imaging the real-time transport into the downstream of lymphatics and blood vessels in mesentery.** Representative intravital images showing the transport of BODIPY-FA (red) via mesenteric collecting lymphatics (arrow) and vein (star). To visualize the vein, Evans blue (blue) was intravenously injected into Prox1-GFP (green) mouse just before the imaging. The representative images were obtained from more than 3 independent experiments. Scale bar, 200  $\mu\text{m}$ .



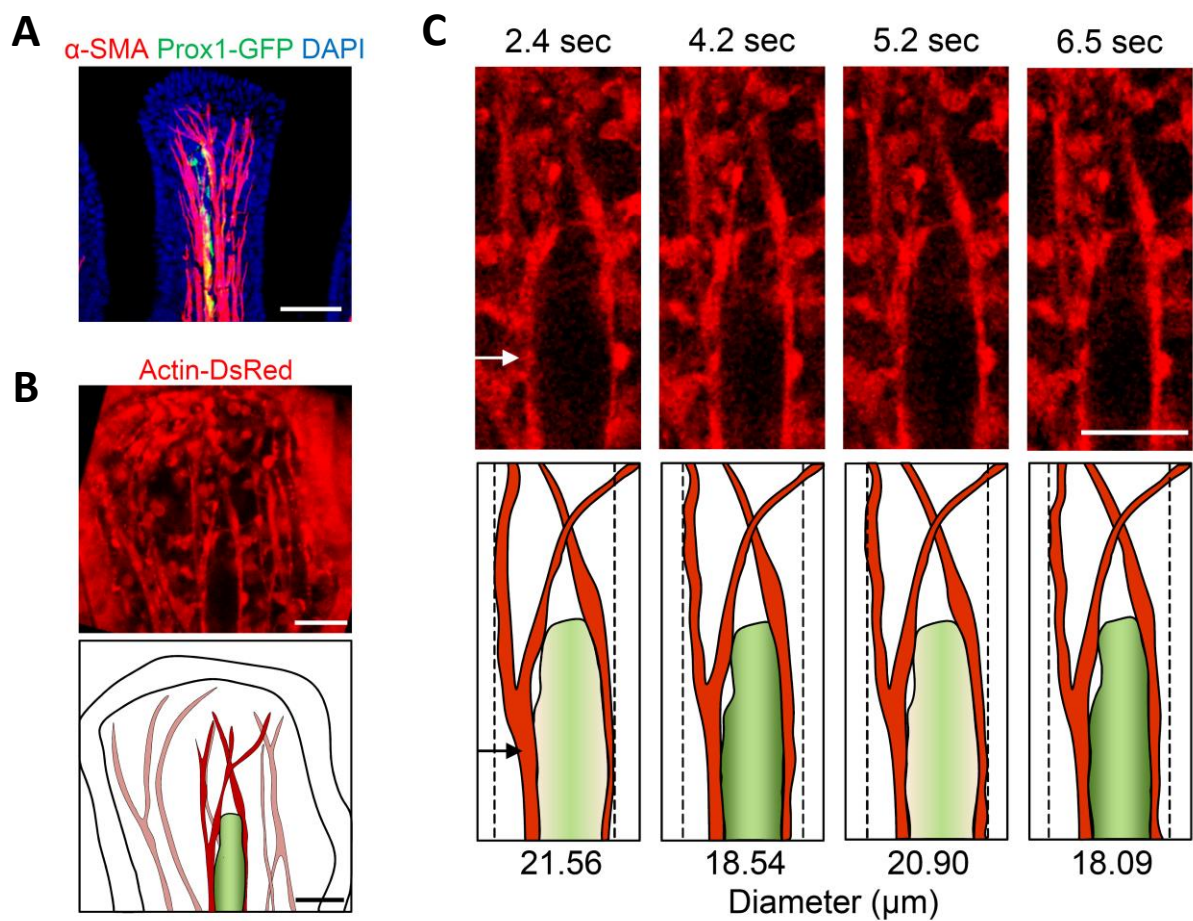
**Supplemental Figure 4. Comparison of speed of C3 FA drainage against that of C12 FA. (A)** Representative intravital images showing the drainage of short chain FA, BODIPY-C3. FA is absorbed into the lacteal (arrow) within 1 min after the first supply and cleared out over the following 2 min. **(B)** Representative intravital images showing the drainage of BODIPY-C12 FA. The representative images were obtained from more than 3 independent experiments each. Scale bars, 30  $\mu\text{m}$ .

**A****B****C****D****E**

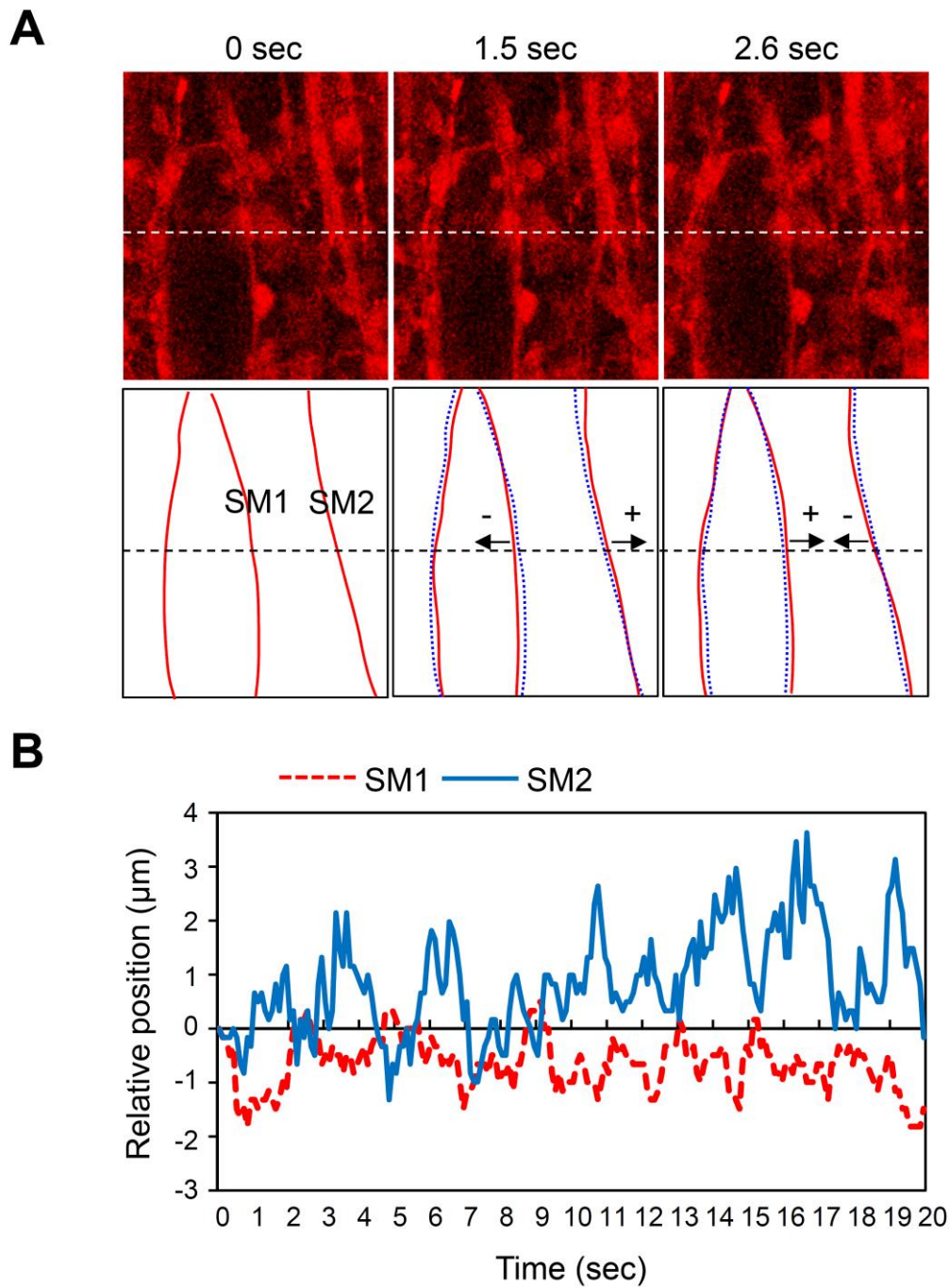
**Supplemental Figure 5. Absorption and drainage of BODIPY-FA C16.** (A) Representative intravital images showing dynamic BODIPY-FA C16 absorption and drainage in a single small intestinal villus. To visualize the lacteal, the wild type FVB/n mouse was intravenously injected with anti-LYVE-1 antibody conjugated with a far-red fluorescence dye, Alexa Fluor® 647, at 12 hr before imaging. (B) Quantification of the average fluorescence intensity (FI) of BODIPY-FA C16 in enterocytes and lacteal. A total of 43 villi from 3 mice were analyzed. Error bars indicate SEM. (C) Representative intravital images showing the delay of C16 FA release from the enterocytes of some villi (Group2) compared with most others (Group1) after the second FA supply. (D-E) Quantification of relative average FI of BODIPY-FA C16 and C12 in the enterocytes and lacteals. A total of 39 and 15 villi from 3 mice were analyzed for C16 group 1 and 2, respectively, and 27 villi from 4 mice were analyzed for C12. \*Significant differences between C16 group1 and 2, #significant differences between C16 group1 and C12,  $P < 0.05$ , non-paired Student's t-test. Error bars indicate SEM. Scale bars, 30  $\mu\text{m}$ .



**Supplemental Figure 6. Intravital imaging of small intestinal villus in early age pups.** BODIPY-C12 FA (orange) is absorbed into the lacteal (green, arrows) within 1 min in mice at postnatal day 0 and day 20. Scale bars, 30  $\mu\text{m}$ .



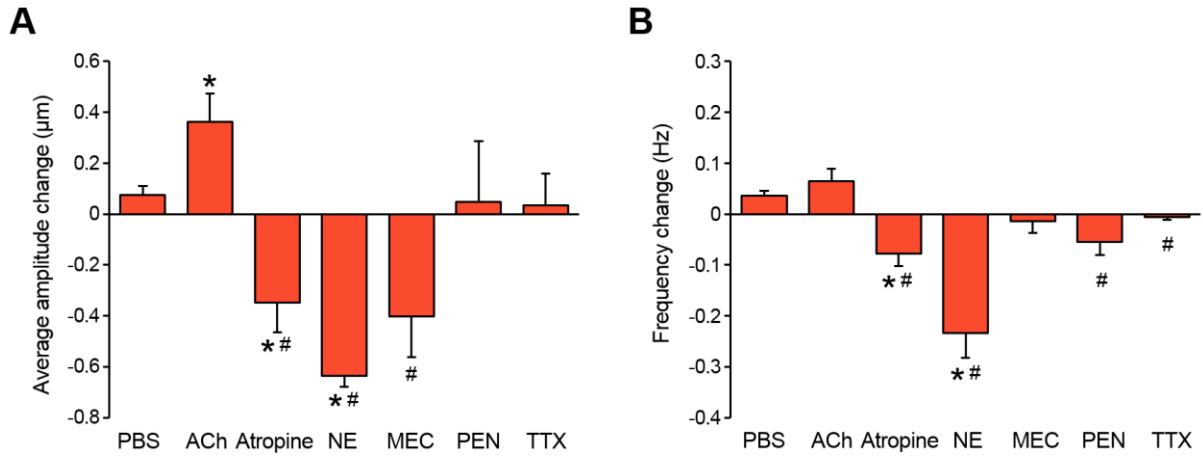
**Supplemental Figure 7. Smooth muscles surround a lacteal in intestinal villi.** (A) A representative immunohistochemistry image of a single villus of a Prox1-GFP mouse stained for  $\alpha$ -SMA and DAPI. Scale bar, 50  $\mu$ m. (B) A representative intravital image (upper panel) and its illustration (lower panel) of a villus of an actin-DsRed mouse. Scale bars, 30  $\mu$ m. (C) Serial video-rating images (upper panels) and their illustrations (lower panels) showing the contractile movements of actin. Lacteal diameters were measured at each time points at the locations indicated in the image (white arrow) and in the illustration (black arrow). Red and green colors represent smooth muscles and lacteal, respectively, in the illustration. Scale bar, 30  $\mu$ m.



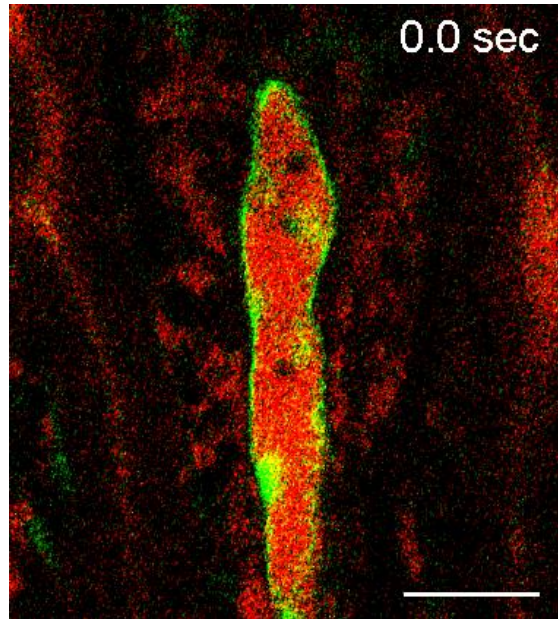
**Supplemental Figure 8.** The smooth muscles that directly surround a lacteal move in a different direction to those that are further away from the lacteal. (A) Serial video-rate images (upper panels) and their illustrations (lower panels) showing the contractile movement of actin. In the illustrations, the blue dotted lines outline the previous position of the smooth

muscles, while the red lines outline the lacteals at the specific time points. The arrows indicate the direction of smooth muscle movements and define the positive and negative directions.

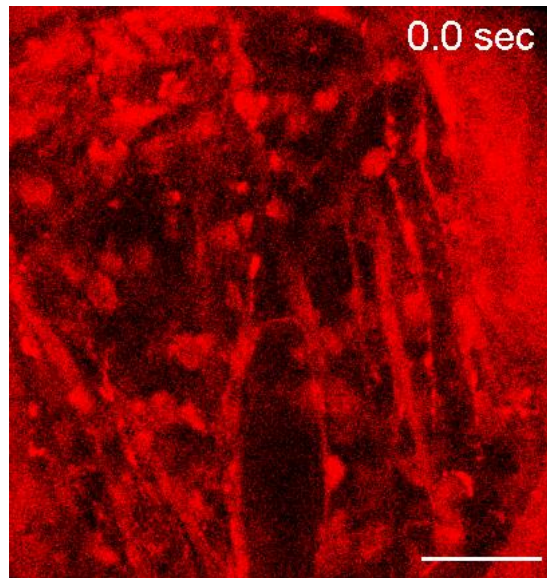
(B) The relative changes in the positions of smooth muscles from their respective initial positions. The positions of smooth muscles were measured along the black dotted line demarcated in (A).



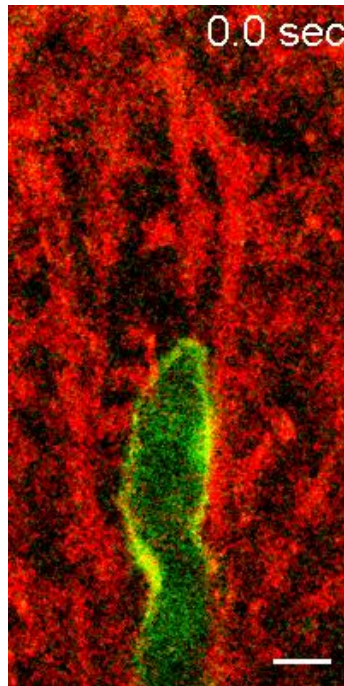
**Supplemental Figure 9. Drug-dependent changes of lacteal contractile motion.** The average amplitude and the frequency of lacteal diameter change were measured before and after administration of drugs onto mesentery region. The numbers of villi that were quantified are 37, 37, and 39 from 4 mice each for PBS, Ach, and mecamylamine (MEC) groups, 47 and 42 from 5 mice each for atropine and norepinephrine (NE) groups, and 26 and 25 from 3 mice for pentolinium (PEN) and tetrodotoxin (TTX) groups, respectively. \*Significant differences between before and after drug administration,  $P < 0.05$ , paired Student's t-test. #Significant differences from PBS group,  $P < 0.05$ , non-paired Student's t-test. Error bars indicate SEM.



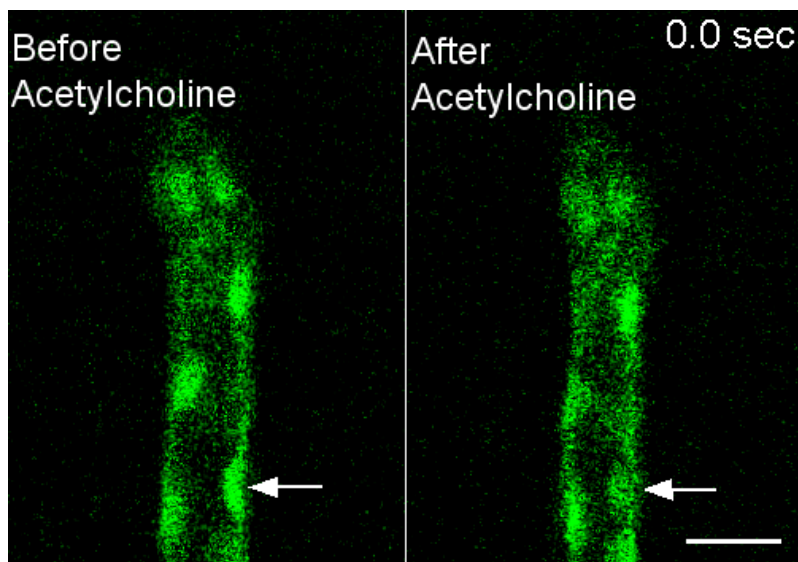
**Supplemental Movie 1.** Real-time movie of lacteal contraction (green) and cell movement (cell shadow made by red BODIPY-FAs in lacteal lumen). Scale bar, 30  $\mu\text{m}$ .



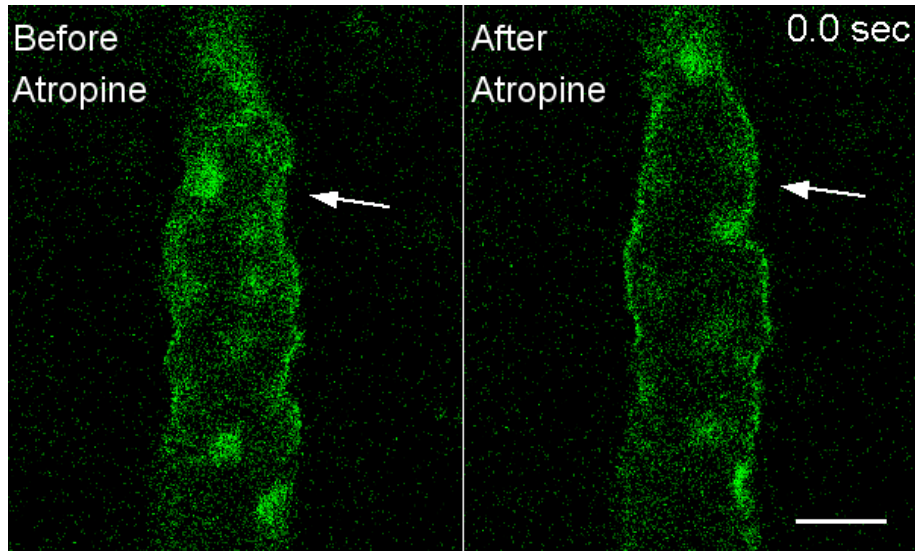
**Supplemental Movie 2.** Real-time movie of smooth muscles contraction adjacent to lacteal of actin-DsRed mouse. Scale bar, 30  $\mu\text{m}$ .



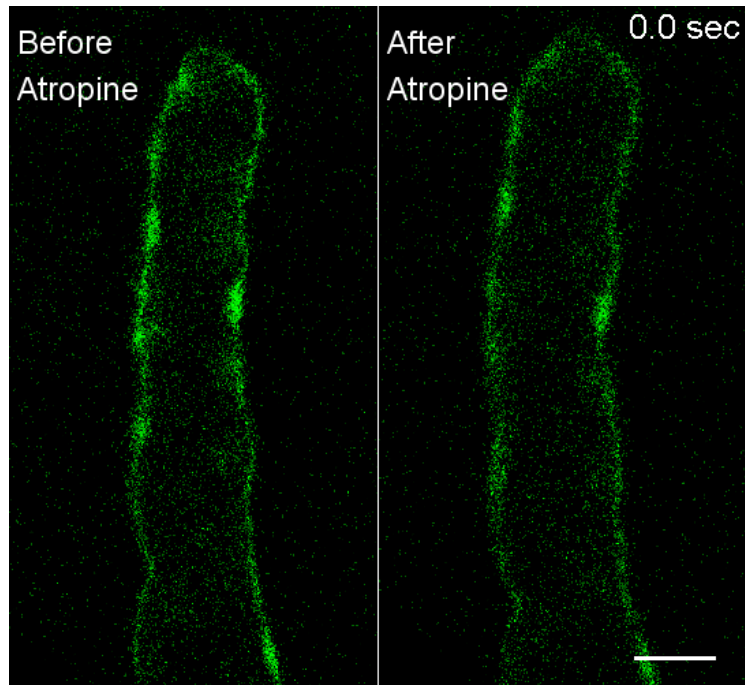
**Supplemental Movie 3.** Real-time movie of smooth muscles (red) and lacteal (green) contraction of a double transgenic mouse (Prox-1 GFP and actin-DsRed). Scale bar, 30  $\mu\text{m}$ .



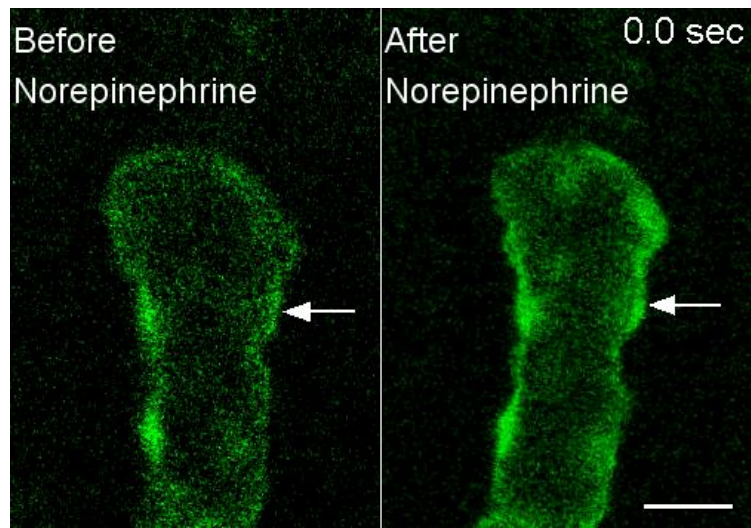
**Supplemental Movie 4.** Real-time movie of lacteal contraction (green) before (left) and after (right) acetylcholine administration. Lacteal diameters were measured at each time points at the locations indicated in the movie (arrows) Scale bar, 20  $\mu\text{m}$ .



**Supplemental Movie 5.** Real time movie of lacteal contraction (green) before (left) and after (right) atropine administration. Atropine attenuated the lacteal contraction particularly in the region indicated by the arrow. Scale bar, 20  $\mu\text{m}$ .



**Supplemental Movie 6.** Real time movie of lacteal contraction (green) before (left) and after (right) atropine administration. Scale bar, 20  $\mu\text{m}$ .



**Supplemental Movie 7.** Real time movie of lacteal contraction (green) before (left) and after (right) norepinephrine administration. Lacteal diameters were measured at each time points at the locations indicated in the movie (arrows). Scale bar, 20  $\mu\text{m}$ .